Urol Res (2007) 35:41–48
DOI 10.1007/s00240-006-0077-x

ORIGINAL PAPER

Analysis of urinary calculi using an infrared microspectroscopic surface reflectance imaging technique

Jennifer C. Anderson · James C. Williams Jr · Andrew P. Evan · Keith W. Condon · André J. Sommer

Received: 18 September 2006 / Accepted: 4 December 2006 / Published online: 5 January 2007

Abstract This investigation highlights the use of infrared microspectroscopy for the morphological analysis of urinary stones. The research presented here has utilized the reflectance mode of an infrared microscope for use in creating chemically specific maps of cross-sectioned renal calculi surfaces, precisely showing the placement of renal stone components in a calculus sample. The method has been applied to renal stones of both single and multiple components consisting primarily of hydroxyapatite, calcium oxalate monohydrate and calcium oxalate dihydrate. Factors discussed include the photometric accuracy of the spectra obtained, a comparison of the surface reflectance method with existing methods such as diffuse reflectance infrared Fourier transform spectroscopy (DRIFTS) and attenuated total internal reflection (ATR) analysis, and the influence of specular reflectance between polished and unpolished sample spectra. Full spectral maps of cross-sectioned renal stones provided positive localization of components using qualitatively accurate spectra similar in appearance to DRIFTS spectra. Unlike ATR and DRIFTS spectra, surface reflectance spectra lack photometric accuracy and are therefore not quantifiable; at present, however, spectra are suitable for qualitative analysis. It was found that specular reflectance increases minimally with a highly polished stone cross-section surface, though qualitative data is not affected. Surface reflectance imaging of sections of renal stones is useful for determining the identity of stone components while simultaneously providing precise locations of mineral components within the stone using presently available instruments.

Keywords Infrared · Urinary calculi · Renal stones · Surface reflectance

J. C. Anderson · A. J. Sommer (✉)
Department of Chemistry and Biochemistry,
Miami University, Oxford, OH 45056, USA
e-mail: sommeraj@muohio.edu

J. C. Williams Jr · A. P. Evan · K. W. Condon
Department of Anatomy and Cell Biology,
Indiana University School of Medicine,
Indianapolis, IN 46202, USA

Introduction

The qualitative and quantitative analysis of intact urinary calculi (stones) is challenging for several reasons, including the size and fragility of the calculi and the spatial domains of their sedimentary chemistry. Many modern methods of analysis destroy the structure of the calculi when the samples are prepared for introduction into the instrument. Maintaining the structural integrity of the calculi is important for the elucidation of the chemistry of formation and the etiology of the calculi in the urinary system.

Understanding the etiology of urinary stones requires analysis not only of their composition, but also of the architectural arrangement of minerals and organic materials in each stone, information that can provide important indicators of the mechanisms of initial formation and subsequent growth of the stone [1–3]. Recent studies have clearly shown that there is more than one pathological pattern for the initiation of calcium stones, [4] and the 3D architecture of early stones will be important for understanding these

different pathological processes and how they result in renal stones [5].

Twenty-four hour urine tests, often used to determine and track urine chemistry in a patient, are helpful for the tracking and treatment of urine/renal system ailments being suffered from at the time of collection [6–8]. However, 24-h urine tests do not indicate past urine chemistry, and are thus unfeasible for the use of determining the chemical etiology or architecture of the renal stones being produced. In order for 24-h urine chemistries to be applied to the long-term determination of renal stone formation, urine chemistry would have to be collected daily over a period of months or years in order to track the changes occurring in the renal system. Additionally, the practitioner would have to possess preemptive knowledge that a renal stone would be formed for that particular patient within the time constraints the 24-h urine test was being undertaken. Taking these facts into consideration, the study of the architecture of renal stones collected from idiopathic calcium stone formers remains the best method for determining the chemistry of formation occurring in the renal system.

Some of the best work on the architecture of stones has utilized thin sections of stones, which are studied by X-ray and/or optical methods [9, 10]. Such studies have elegantly shown the nature of the progressive addition of layers to stones, and have also attempted to identify the nucleus, or initial nidus of the stones. Related work has also been done using micro dissection of stones with analysis of samples by infrared (IR) spectroscopic methods [3]. Additionally, several reports have been published on the comparison of IR techniques to wet chemical methods for renal stone and other biological analysis, though these can be somewhat outdated [11–13].

Recent IR imaging studies have focused on isolated areas of calcified tissue and bone sections. The majority of these studies have employed transmission methods of analysis, which require the sample to be present as thin sections approximately 6 μm thick [14–18]. Several of these reports study thin sections of bone, which are structurally more robust than thin sections of urinary calculi [18, 19]. Thin sections of reproducible thickness are difficult to obtain with urinary stones because of the fragile nature of the material [9, 10].

In a report previously published by this laboratory, [20] we demonstrated the feasibility of using reflection/absorption infrared (RAIR) and attenuated total internal reflection (ATR) microspectroscopy as a technique for the qualitative analysis of tissue sections containing embedded mineral deposits. In addition to the qualitative analysis of these mineral deposits, reflectance IR microspectroscopic techniques can also be used to determine the composition of cross-sectioned urinary calculi—more durable than thin sections—which is the topic of this report.

Reflectance spectroscopy includes both specular and diffuse measurements; however, each method requires that the sample have specific properties. For specular reflectance, the surface of the sample must be similar to that of a dielectric material (e.g., polycarbonate) [21]. The spectra collected typically exhibit absorptions resembling the first-derivative of a normal absorption band. These spectra can be corrected for such asymmetric features using the well-known Kramers–Kronig transformation. Therefore, a specular reflectance spectrum can be transformed into an apparent transmission spectrum [22]. Although specular reflectance IR microspectroscopy could be employed, this method also requires significant sample preparation [23].

Diffuse reflectance spectroscopy requires that the sample be a highly scattering powder with individual particle sizes that approach the wavelength of radiation being employed in the analysis. Radiation enters the sample and re-emerges after traveling a complex path through the sample. During the residence time in the sample, the radiant energy experiences a myriad of phenomena which can include diffraction, reflection, refraction, scattering, and absorption [24]. Theoretically, as the particle size increases relative to the wavelength of light, the sample surface appears more mirror-like, increasing the amount of specular reflection.

Currently, diffuse reflectance Fourier transform infrared spectroscopy (DRIFTS) is widely used in urological analysis. Unfortunately, this method requires the sample to be ground to a fine powder and diluted with potassium bromide thereby destroying the stone. Although DRIFTS can yield qualitative and quantitative results, the preparation of the calculi samples is time consuming and difficult. For the analysis of a renal stone, each individual layer must be physically separated from the main body of the stone. This method has the potential to introduce significant error since the layers are often not uniform with respect to composition or their coverage of the calculus and can often be quite thin [9].

With these considerations in mind, we present a facile method of analysis for isolated cross-sectioned urinary calculi, either unmounted or stabilized in resin. A cross-sectioned stone, regardless of thickness, can be analyzed using the reflectance mode of an IR microscope, yielding spectra that are qualitatively accurate and are similar in appearance to DRIFTS spectra. In addition to the qualitative IR microspectroscopic analysis of urinary calculi components, we also present a study of the effects of surface roughness on IR reflectance spectra.

Materials and instrumentation

Intact human urinary calculi were obtained as discards from a stone analysis laboratory, and were embedded in methyl methacrylate. Calculi cross-sections 1–2 mm thick were cut using a diamond wire saw (Well Saw, Delaware Diamond Knives, DE) and were mounted onto low-E glass slides for subsequent analysis.

Rabbit femur cross-sections were obtained as discards from appropriately approved animal work done by other laboratories. Serial cross sections were alternately embedded in methyl methacrylate or left unmounted. Both embedded and loose bone sections were polished using a series of silicon carbide abrasive media possessing a grit size from 16 to 0.05 μm. This procedure yielded samples ranging from unpolished wire-cut surfaces to highly polished surfaces.

The DRIFTS spectra of ground reference materials presented in this report were collected using the Perkin-Elmer Spectrum Spotlight 300 IR imaging microscope equipped with a single point HgCdTe (MCT) detector, and represent the average of 32 individual scans collected at a spectral resolution of 4 cm^{-1}. A 25 × 25 μm confocal aperture was employed to isolate the sample region of interest for both the DRIFTS and reflectance experiments when single point detection was used. Background spectra were collected using ground potassium bromide (KBr) as the reference material.

Images of sectioned calculi and bone were collected on the Perkin-Elmer Spectrum Spotlight 300 IR imaging microscope using the linear array MCT detector. Spectra collected and extracted from false-color images using this detector represent the average of eight scans at a spectral resolution of 8 cm^{-1}. Each spatial element on this detector represents 6.25 × 6.25 μm^2 area on the sample. Background spectra were collected using the reflective side of a low-E slide.

ATR spectra were collected on the Perkin-Elmer Spectrum Spotlight 300 IR imaging microscope using the drop-down Ge internal reflection element (IRE) and the single point MCT detector. Spectra collected represent the average of 32 scans with a spectral resolution of 4 cm^{-1}. Background spectra were collected using a KCl pellet as the reference material.

Results and discussion

A renal stone sample, encased in resin and sliced to a thickness of several millimeters, is utilized by medical researchers due to the fact that this sample configuration retains its physical features for analysis. By studying the radial projection of cross-sectioned urinary calculi, it is possible to determine the chemistry from nucleation to some arbitrary point in time. The nucleation and growth process of urinary calculi are similar to the geochemistry of sedimentary layers associated with the earth, but with the time and distance scales being highly compressed. IR imaging of cross sectioned urinary calculi allows one to precisely obtain molecular information as a function of position and therefore time enabling one to determine the chemistry of calculi formation.

Due to their importance and relative abundance, renal stones containing calcium oxalate and/or calcium hydroxyapatite are the focus of this investigation. Figure 1 illustrates a 6.5 × 9.0 mm cross-sectioned calculus composed of calcium oxalate and hydroxyapatite. The physical features of the stone include the radial distribution of the component layers in irregular patterns and varying colors. The varying colors in the radial distribution are not necessarily indicative of component differences, though quite often this is the case [25]. The outlined box in Fig. 1 contains several bands of varying color as well as a portion of an innermost region. This sampling of the renal stone appears to be representative of a radial projection of the entire stone. Figure 2 illustrates false color images of the selected area, generated from ~130,000 spectra collected over a nearly 7 h time frame. The spectra were collected using a linear array detector with a pixel size corresponding to a 6.25 × 6.25 μm spatial element on the sample. Background spectra were

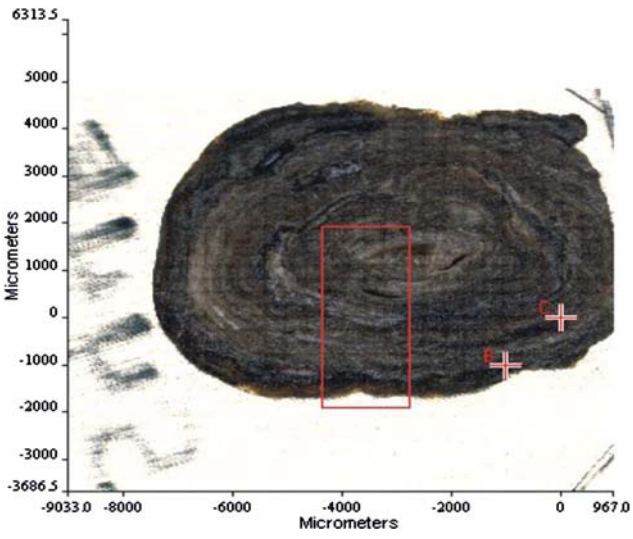

Fig. 1 Visible image of a cross-sectioned renal stone containing radial projections of differing components. The area of interest is outlined by a *box* containing a varied sampling of the components present in the section

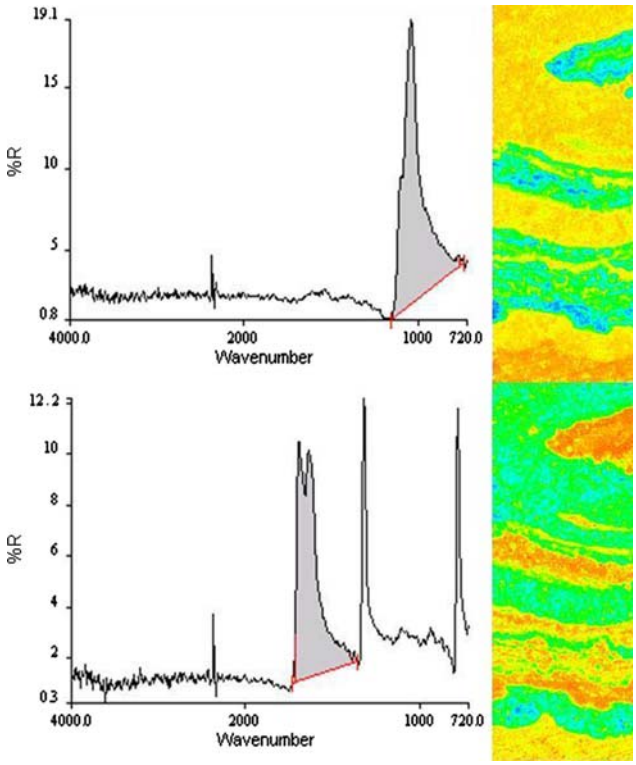

Fig. 2 Infrared image maps of the outlined area in Fig. 1 and associated spectra of a cross-sectioned renal calculus. *Top* calcium hydroxyapatite. *Bottom* calcium oxalate. *Blue/green* indicates the presence of the component, while *red/yellow* indicates a lack of the specified component

collected every five points to maintain good atmospheric compensation during the course of the nearly 7 h analysis period. To reduce the time period required for analysis, spectral resolution can be lowered slightly, or the area selected for analysis diminished in size. The slight lowering of the spectral resolution is acceptable due to the purely qualitative nature of the method.

Each spatial element in the mapped region is associated with a complete IR spectrum ranging from 4,000 to 700 cm^{-1} that can be viewed separately or combined as a molecular (component) specific image. For example, the spectra illustrated in Fig. 2 were used to create false color images using total absorbance of specified spectral features. The top panel shows a spectrum characteristic for hydroxyapatite; the main feature located near 1,020 cm^{-1} is due to the asymmetric stretch (ν_{as}) of the orthophosphate group in apatite. The false color map in the top panel shows the component specific image obtained using the integrated band intensity near 1,020 cm^{-1}. Areas with a greater abundance of hydroxyapatite are indicated by the blue/green colors corresponding to a higher integrated intensity; areas shaded red/yellow indicate the absence of hydroxyapatite and/or the presence of another material. The image demonstrates that the innermost layer of this section of the stone is composed of hydroxyapatite.

The composition in the outer extremity of the stone can be determined by extracting a spectrum from this region, and was found to correspond to calcium oxalate. The lower panel of Fig. 2 illustrates a spectrum characteristic of calcium oxalate. Features observed in this spectrum are due to the asymmetric stretch of the oxalate anion (ν_{as}) located near 1,624 cm^{-1}, the symmetric stretch of the oxalate anion at 1,321 cm^{-1} and the C–O bend located near 785 cm^{-1}. A map of the calcium oxalate content of this section is shown in the right of the lower panel, based on the intensity of the peak near 1,624 cm^{-1}. Again, blue/green indicates a high prevalence of the calcium oxalate material, while red/yellow indicates its absence.

A closer inspection of calcium oxalate spectra reveals that two different hydrates are present in this stone. These two hydrates consist of calcium oxalate monohydrate (COM) and calcium oxalate dihydrate (COD). The two materials are readily distinguished by the position of the asymmetric oxalate anion stretch. For COM this band is located at 1,624 cm^{-1}, and for the COD, it is located near 1,680 cm^{-1}. The 1,321 and 785 cm^{-1} bands remain the same for both oxalate species. Figure 3 displays false color maps of COM (top panel) and COD (bottom panel) for this region of the stone section, indicating the variability in hydrate content in different layers of the stone. These differences are detected using a 56 cm^{-1} wavenumber difference between COM and COD and demonstrate the chemical specificity of IR spectroscopy.

The compositional complexity of the stone section shown in Figs. 1, 2, and 3 is quite a common finding in renal stones, [3, 9] and the general lack of recognition of such complexity is a possible reason for the generally poor performance of stone analysis facilities. A standardized test system in the UK has shown an average error rate of 30–40% in standard samples analyzed by commercial laboratories [26]. Looking at the maps of composition in Figs. 2 and 3, it can be seen how the portion of the stone taken for analysis could easily imply a result of hydroxyapatite or COM or dihydrate, dependant upon the portion analyzed. Or, a single sampling could imply a result that would indicate a mixture of all three minerals. Therefore it is imperative that multiple sites be analyzed throughout the sample stone, thereby providing a full understanding of the stones chemistry.

A concern appropriate to renal stone analysis may be the inclusion of proteinaceous material in the

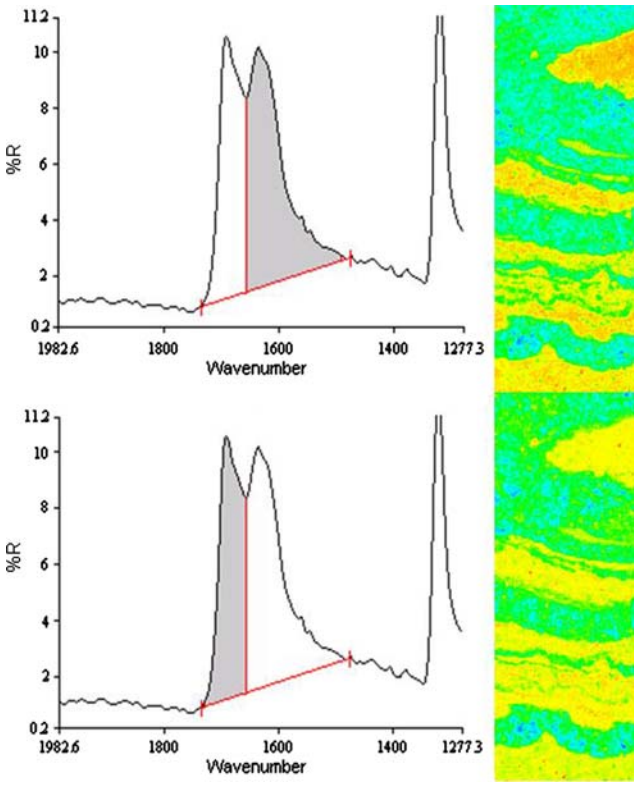

Fig. 3 Full spectral infrared image maps and associated spectra of the two hydrates of calcium oxalate. *Top* calcium oxalate monohydrate. *Bottom* calcium oxalate dihydrate

sample. Though dehydration and embedding process is undergone, protein residue may remain in the body of the calculus. Unfortunately, the quantitation of COM in the presence of protein is difficult due to the close proximity of the 1,633 cm^{-1} amide I band of protein to the 1,624 cm^{-1} ν_{as} C=O stretching band of oxalate. Due to this encroachment, molecular image maps obtained of the sample often lack qualitative and quantitative properties when the 1,624 cm^{-1} absorbance band of COM is used if protein is present. Therefore, the absorption band of oxalate at 778 cm^{-1}, the O–C–O bend, and the ν_s C=O stretch at 1,318 cm^{-1} are used for most qualitative and semi-quantitative measurements. Additionally, though they are not overlapping, the amide III band from protein lies in close proximity to the oxalate 1,318 cm^{-1} ν_s C=O band, and should be taken into consideration in quantitative measurements concerning the 1,318 cm^{-1} oxalate band. However, the presence of protein does not interfere with the identification or quantitation of calcium hydroxyapatite.

Figures 2 and 3 demonstrate that the composition of consecutive layers of mineral in a renal stone can be determined using IR reflectance imaging. Two important questions concerning these results are: (1) would better sample preparation help and (2) would another measurement mode be preferable? It is known that polished surfaces, such as those of a dielectric sample, often result in greater surface reflectance than unpolished surfaces [27]. To attempt to determine if specular reflectance increases with a more highly polished renal stone sample, individual renal stones were gently hand polished using sandpaper varying from 16 to 0.05 μ in grit size. However, polishing the surface of the fragile renal calculi frequently led to their disintegration. As an alternative, bone cross sections were polished to varying degrees utilizing the same range of abrasive media in order to test this first question. Bone was chosen as an acceptable substitute since, spectroscopically, the intensity and band shape of the main hydroxyapatite band at 1,020 cm^{-1} for bone and renal calculi were observed to be nearly identical, as shown in Fig. 4.

Figure 4 displays spectra corresponding to hydroxyapatite from both bone (solid) and a cross-sectioned renal stone (dashed). As can be seen, the spectra are qualitatively similar, and both spectra show low peak-to-peak noise. Spectra of bone, polished using 0.05 μ grit sanding paper and embedded in resin, exhibited a peak-to-peak noise of 0.66 whereas that of the wire-cut stone was 0.53. Polished and unpolished bone sections were imaged using the reflectance mode of the IR microscope in a manner identical to that of the renal calculi samples. Spectra of highly polished (0.05 μm surface roughness) bone sections and unpolished, wire-cut bone sections are compared in Fig. 5. The results show minimal differences between the spectra with respect to reflected intensity and peak-to-peak noise. The absorption band intensity of the polished cross section (dashed) is slightly larger than that of the unpolished section (solid) by approximately five units. This slight intensity difference is probably due to the lack of scattering from the polished surface compared to the more diffuse nature of the surface of the wire-cut bone sample. The data suggest that improvements with additional polishing are negligible and that the surface characteristics of the calculi and bone do not affect the reflectance process greatly.

To answer the second question, a comparison of COM spectra obtained with ATR, surface reflectance and diffuse reflectance IR microspectroscopy using identical conditions other than measurement mode is shown in Fig. 6. The spectra show minimal differences with regard to both band shape and positioning, though signal to noise ratio is much higher for DRIFTS (top) and ATR (middle) than for the surface reflectance (bottom) method. Upon close inspection of the surface reflectance spectrum in Fig. 6, it can be seen that the group of bands from 3,400 to 3,000 cm^{-1} attributed to the symmetric and asymmetric OH stretch of crystallized water

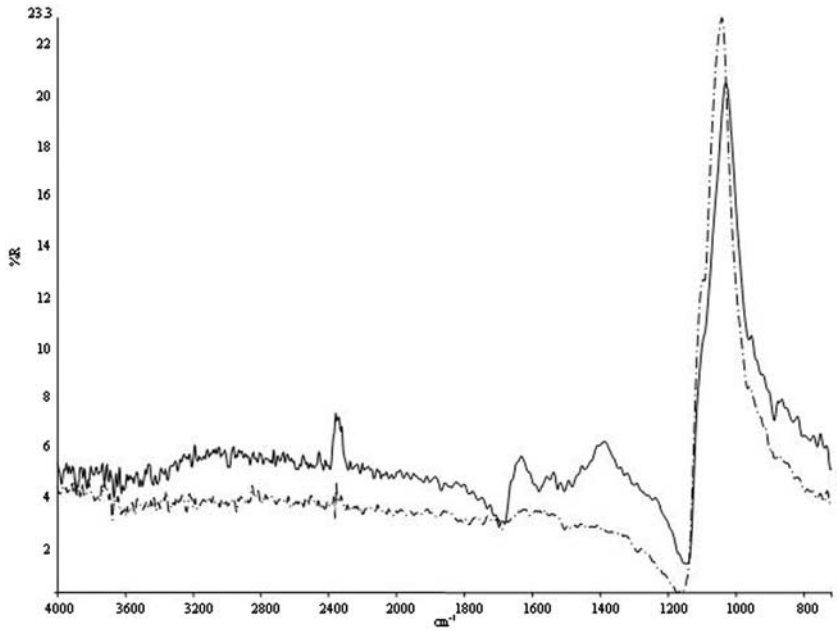

Fig. 4 Comparison between spectra taken from a bone cross-section (*solid line*) and a renal stone cross-section (*dashed line*). Observed and collected under identical surface reflectance conditions

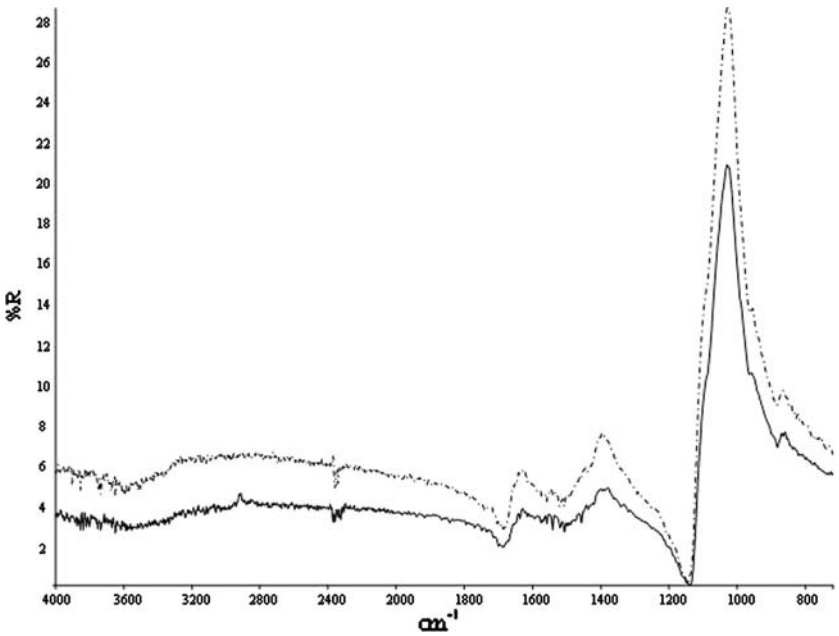

Fig. 5 Comparison between highly polished (*dashed line*) and unpolished/wire-saw cut (*solid line*) bone cross-sections. Observed and collected under identical surface reflectance conditions. Polishing occurred using 0.05 μm grit sand paper

[28], the shoulder at 1,375 cm^{-1} attributed to the symmetric stretch of the oxalate anion [29], and two weaker bands at 884 and 945 cm^{-1} attributed to OH deformation [29] of COM are absent. Additionally, these bands are greatly diminished in the ATR spectrum of COM oxalate monohydrate. The absence of these bands in the surface reflectance spectrum are due to a combination of factors, including the crystalline structure of the stone but most importantly the optical characteristics (e.g., refractive index) of the material. The low absorbance observed in the surface reflectance spectrum is an indicator that the probe beam penetrates the surface only slightly resulting in a reduced optical path length. On the other hand, the high absorbance associated with the bands in the diffuse reflectance spectrum result from a greater optical path length. For diffuse reflectance, a small amount of sample is mixed with an IR transparent sample like KBr. Due to the nature of the sample, multiple scattering events take place, which increase the optical path length for a given sample. ATR on the other hand is intermediate, and the optical path length increases from the high-energy end of the spectrum to the low-energy end. At the high-energy end the optical path length is less than 0.39 μm and increases to 2.14 μm toward the low-energy end. This change is why the features located near 3,200 cm^{-1} have reduced intensity

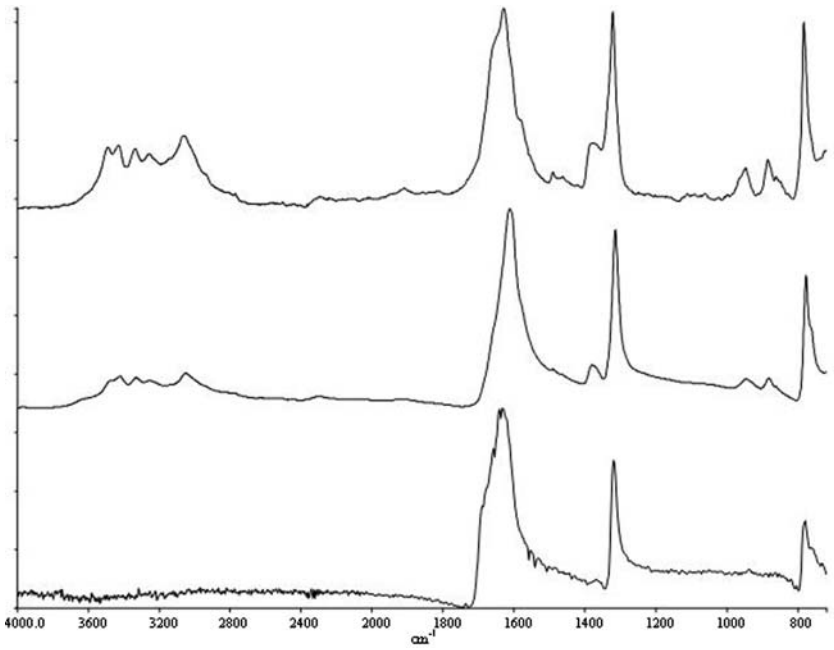

Fig. 6 Comparison between DRIFTS (*top*), ATR (*middle*) and surface reflectance (*bottom*) spectra of calcium oxalate monohydrate

in the ATR spectrum but those at 945 and 884 cm^{-1} are clearly visible.

With regard to photometric accuracy, that is, the linear relationship between band absorbance and optical path length, both DRIFTS and ATR spectra can be photometrically accurate. As a result these methods can be used in a semi-quantitative capacity. However, it has yet to be determined whether surface reflectance spectroscopy can be used in a quantitative capacity (photometrically correct). Surface reflectance and ATR methods are complementary reflectance techniques, each possessing certain strengths. Analysis utilizing the surface reflectance microspectroscopic technique is fast and requires limited sample preparation allowing a diversity of samples to be analyzed. However, due to scattering, reflection, refraction, and sample topography, quantitative information may be difficult to extract. Under most conditions, ATR produces photometrically accurate bands capable of yielding quantitative data with a high signal to noise ratio [30]. Unfortunately, this method requires sample contact with the IRE. This contact could potentially damage the sample, and in the case of unstable samples, the IRE may need to be cleansed in between successive sample points. Therefore the process of creating a spectral map of a sample using ATR is time consuming and requires constant involvement by the operator. The method most applicable and successful for sample analysis is to use the two techniques in conjunction with one another. A full spectral map can quickly be made of the sample, highlighting features of interest and determining general homogeneity. Earlier research by this laboratory has confirmed that subsequent analysis using ATR microspectroscopy yields photometrically accurate data suitable for the extraction of quantitative information [20].

Though the data provided in this research pertains to a single stone cross-section, similar successful data has been accumulated for over 30 renal stone cross-sections in this laboratory. The majority of renal stones examined contain calcium oxalates and/or hydroxyapatite, with many exhibiting the concentric ring structure displayed here. Other compounds investigated in the course of this research include struvite, brushite and cystine. Future research will include different morphologies and additional varieties of renal stones.

Attempts to improve the quantitative analysis will be attempted using off-axis ATR imaging [31], which combines the ease of molecular imaging via surface reflectance with the photometric accuracy achievable by ATR methods. Using this method, the renal stone sample will retain its original form for the elucidation of stone formation data with minimal preparation identical to that of the surface reflectance method presented in this research. The time taken for total analysis would be greatly reduced since the molecular image map would be quantitative in character, making subsequent follow-up analysis via conventional ATR unnecessary.

Conclusion

We have presented here a facile method for qualitative, spatial analysis of the mineral layers in a section of

urinary stone using instrumentation and software that are easy to use. This method is less susceptible to error or misdiagnosis than common methods of stone analysis, and bypasses the sectioning and grinding steps that have been required for analysis of sections of urinary calculi in the past. In addition, we have provided evidence that an unpolished sample yields similarly informative spectra to that of polished sections, supporting our assertion that no extensive sample preparation is needed to obtain high quality qualitative spectra and molecular maps using the IR microspectroscopic reflection technique.

Unfortunately, the above research is not quantitatively valid due to the lack of photometrically accurate absorption bands. It may be a regretful fact that surface reflectance proves thus far to be solely qualitative in nature without the aid of subsequent ATR analysis. However, current research in our laboratory is focusing on quantitative methods of cross-sectioned stone analysis utilizing off-axis ATR methods that will yield photometrically accurate spectra with the ease and full spectral map capabilities of surface reflectance. In future research, a large hemispherical IRE in direct contact with a cross-sectioned renal stone will be used in an attempt to achieve timely, resolved, and photometrically accurate IR maps capable of yielding qualitative as well as quantitative data.

Acknowledgments The authors would like to thank Molly Jackson for her aid in the acquisition and preparation of the urinary calculi samples. Additionally, funding for a portion of this research was obtained from the National Institute of Health, grant PO1 DK56788.

References

1. Sperrin MW, Rogers K (1998) Br J Urol 82:781–784
2. Daudon M (2004) Rev Med Suisse Romande 124:445–453
3. Daudon M, Bader CA, Jungers P (1993) Scanning Microsc 7:1081–1106
4. Evan A, Lingeman J, Coe FL, Worcester E (2006) Kidney Int 69:1313–1318
5. Williams JC, Matlaga BR, Kim SC, Jackson ME, Sommer AJ, McAteer JA, Lingeman JE, Evan AP (2006) Calcium oxalate calculi found attached to the renal papilla: preliminary evidence for early mechanisms in stone formation. J Endourol 20(11):885–890
6. Williams CP, Child DF, Hudson PR, Davies GK, Davies MG, John R, Anandaram PS, De Bolla AR (2001) J Clin Pathol 54:54–62
7. Stitchantrakul W, Sopassathit W, Prapaipanich S, Domrongkitchaiporn S (2004) Southeast Asian J Trop Med Public Health 35:1028–1033
8. Chai W, Liebman M, Kynast-Gales S, Massey L (2004) Am J Kidney Dis 44:1060–1069
9. Murphy BT, Pyrah LN (1962) Br J Urol 34:129–159
10. Cifuentes DL (1977) J Urol Nephrol 83(Suppl 2):592–596
11. Gault MH, Ahmed M, Kalra J, Senciall I, Cohen W, Churchill D (1980) Clin Chim Acta 104:349–359
12. Volmer M, DeVries J, Goldschmidt H (2001) Clin Chem 47:1287–1296
13. Carmona P, Bellanato J, Escolar E (1997) Biospectroscopy 3:331–346
14. Ouyang H, Paschalis E, Mayo W, Boskey A, Mendelsohn R (2001) J Bone Miner Res 16:893–900
15. Paschalis E, Verdelis K, Doty S, Boskey A, Mendelsohn R, Yanauchi M (2001) J Bone Miner Res 16:1821–1828
16. Gadaleta S, Landis W, Boskey A, Mendelsohn R (1996) Connect Tissue Res 34:203–211
17. Mendelsohn R, Paschalis E, Sherman P, Boskey A (2000) Appl Spectrosc 54:1183–1191
18. Mendelsohn R, Paschalis E, Boskey A (1999) J Biomed Opt 4:14–21
19. Boskey AL, Gadaleta S, Gundberg C, Doty SB, Ducy P, Karsenty G (1998) Bone 23:187–196
20. Anderson JC, Dellomo J, Sommer AJ, Evan AP, Bledsoe S (2005) Urol Res 33:213–219
21. Bergin FJ (1989) Appl Spectrosc 43:511–515
22. Kubelka P, Munk MP (1931) Z Tech Phys 12:593
23. Rintoul L, Fredericks PM (1995) Appl Spectrosc 49:608–616
24. Blitz JP (1998) Diffuse reflectance spectroscopy. In: Mirabella FM (ed) Modern techniques in applied molecular spectroscopy. Wiley, New York
25. Kleeberg J, Gordon T, Kedar S, Dobler M (1981) Urol Res 9:259–261
26. Kasidas GP, Samuell CT, Weir TB (2004) Ann Clin Biochem 41:91–97
27. Lippert RJ, Lamp BD, Porter MD (1998) Specular reflection spectroscopy. In: Mirabella FM (ed) Modern techniques in applied molecular spectroscopy. Wiley, New York
28. Tomar VS, Bist HD (1970) Appl Spectrosc 24:598–601
29. Bellamy LJ (1966) The infra-red spectra of complex molecules. Wiley, New York
30. Mirabella FM (1998) In: Mirabella FM (ed) Attenuated total reflection spectroscopy, in modern techniques in applied molecular spectroscopy. Wiley, New York
31. Patterson BM, Havrilla GJ (2006) Attenuated total internal reflection infrared microspectroscopic imaging using a large-radius germanium internal reflection element and a linear array detector. Appl Spectrosc 60(11):1256–1266